knowing the effective elastic and damping properties of the materials over a sufficiently large frequency range the speed and attenuation of the pulses can be predicted using the linear theory of viscoelasticity.

Material dispersion appears to be relatively insignificant in glass-epoxy and boron-epoxy samples below 0.25 mHz, although further research in this area is needed. Ultrasonic methods have been shown to provide a useful way of studying dispersion in composite materials.

In this paper attention has been restricted to disturbances propagating in the direction of the reinforcing filaments. A complete characterization of the dynamic behavior of unidirectional fiber-reinforced materials requires a knowledge of the remaining four dynamic moduli (assuming transverse isotropy). Hence additional testing is needed.

References

[1] Schultz, A. B. and Tsai, S. W., "Dynamic Moduli and Damping Ratios in Fiber-Reinforced Composites," *Journal of Composite Materials*, Vol. 2, 1968, p. 368.

[2] Schultz, A. B. and Tsai, S. W., "Measurements of Complex Dynamic Moduli for Laminated Fiber-Reinforced Composites," *Journal of Composite Materials*, Vol. 3, 1969, p. 434.

[3] Abbott, B. W. and Broutman, L. J., "Stress-Wave Propagation in Composite Materials," *Experimental Mechanics*, Vol. 6, 1966, p. 383.

[4] Lifshitz, J. M., "Specimen Preparation and Preliminary Results in a Study of the Mechanical Properties of Fiber Reinforced Materials," MML Rept. 15, Jan. 1969, Israel Inst. of Technology.

[5] Kolsky, H., "The Propagation of Stress Pulses in Viscoelastic Solids," *Philosophical Magazine*, Vol. 1, 1956, p. 693.

[6] Bodner, S. R. and Kolsky, H., "Stress Wave Propagation in Lead," *Proceedings of the 3rd U.S. National Congress of Applied Mechanics*, 1958, p. 495.

[7] Asay, J. R., Dorr, A. J., Arnold, N. D., and Guenther, A. H., "Ultrasonic Wave Velocity-Temperature Studies in Several Plastics, Plastic Foams and Nose-Cone Materials," AFWL-TR-188, March 1966, Air Force Weapons Lab.

[8] Asay, J. R., Urzendowski, J. R. and Guenther, A. H., "Ultrasonic and Thermal Studies of Selected Plastics, Laminated Materials, and Metals," AFWL-TR-67-91, Jan. 1968, Air Force Weapons Lab.

[9] Timoshenko, S., Vibration Problems in Engineering, 3rd ed., D. Van Nostrand, New York, 1955, p. 334.

[10] Pao, Y. H. and Kowal, C., "A Laboratory for Teaching Mechanical Vibrations," *Journal of Engineering Education*, Vol. 56, 1965, p. 96.

[11] Kolsky, H., "Viscoelastic Waves," *International Symposium on Stress Wave Propagation in Materials*, edited by N. Davids, Interscience, New York, 1960, p. 59.

[12] Kolsky, H., "The Propagation of Mechanical Pulses in Anelastic Solids," *Behavior of Materials under Dynamic Loading*, edited by N. J. Huffington, Jr., ASME, 1965.

[13] Kolsky, N., *Stress Waves in Solids*, Dover, New York, 1963, p. 54.

AUGUST 1971 AIAA JOURNAL VOL. 9, NO. 8

Crossflow and Unsteady Boundary-Layer Effects on Rotating Blades

H. A. DWYER*
University of California, Davis, Calif.

AND

W. J. MCCROSKEY†
U. S. Army Aeronautical Research Laboratory, Moffett Field, Calif.

Laminar viscous flow on propellers and helicopter rotors has been studied for a wide variety of blade shapes and environments. The significance of crossflow and unsteady effects has been assessed, and the physical processes which influence the primary flow around the blade have been explained. Special attention has been devoted to those terms in the differential equations that change the boundary-layer structure from that of two-dimensional steady flow. Detailed analyses and calculations reveal that large rotational effects are limited to the immediate vicinity of the rotor hub, while the unsteady and yawed-wing effects of forward flight are important over most of the blade surface. However, chordwise pressure gradients tend to predominate over rotational and unsteady velocity effects for blunt bodies or thin airfoils at large angles of attack. Experimental results for laminar separation and transition support these predictions.

I. Introduction

SOME of the least understood and most important problems in fluid flow are associated with the three-dimensional and time-dependent environments that exist in the real world. The reasons for this lack of understanding are basically twofold: 1) there is a general lack of analytical and numerical techniques available which can handle three-dimensional and time-dependent problems; and 2) experimental measurement techniques are primarily two-dimensional and steady. In this paper the important practical problem of boundary-layer flow over a helicopter rotor is tackled analytically and experimentally. The rotor problem has many three-dimensional features in common with geophysical flows, turbine blades, propellers and rotating machinery, and it also contains a strong time-dependent characteristic. Therefore, a fundamental attack on the helicopter rotor problem is of general interest to many areas of fluid dynamics.

The problems involved with helicopter rotors can best be explained with the help of Fig. 1. The most general rotor

Presented as Paper 70-50 at the AIAA 8th Aerospace Sciences Meeting, New York, Jan. 19–21, 1971; submitted February 20, 1970; revision received January 25, 1971.

Index Categories: Rotary Wing and VTOL Aerodynamics; Boundary Layers and Convective Heat Transfer—Laminar; Nonsteady Aerodynamics.

* Associate Professor, Member AIAA.

† Research Scientist, Member AIAA.

environment exists for forward flight conditions, and in forward flight the flow over the blade will be due to the following: 1) a constant angular velocity of the rotor blades, Ω; 2) a constant velocity, V_1, due to forward flight, which approaches the blade in its plane of rotation; 3) an approximately constant velocity, V_2, due to induced flow through the rotor, which approaches the blade normal to its plane of rotation; and 4) downwash vorticity due to the wake of the previous blade. The angular velocity, Ω, causes the rotational effects on the blade, such as the Coriolis and centrifugal forces that arise in blade-fixed coordinates. The forward flight velocity, V_1, combined with the rotational motion, causes the flow over a helicopter rotor to be unsteady (this should be distinguished from the unsteadiness caused by changing the angle of attack when going from the advancing to retreating blade portions of the rotor disc). The inflow velocity, V_2, influences the local angle of attack and the slipstream contraction, but these are purely inviscid phenomena and add no extra complication to the viscous flow. On the other hand, the trailing vorticity in the wake can produce locally large changes in flow direction and angle of attack that are important in the boundary layer as well as in the potential flow.

Most of the previous analytical work on laminar boundary-layer flow on rotating blades was done by Sears and his coworkers[1-7] in the 1950's and was treated within the framework of the small-crossflow approximation. Because of limitations inherent to the small-crossflow method, the previous analyses were not capable of treating accurately real airfoil shapes nor the regions near the hub where experiments, such as Himmelskamp's,[8] show large rotational effects. Another attempt to solve the hover problem has been recently published by Warsi;[9] however, from the present analysis and that of previous workers, it seems that this work is incorrect. The first analytical attack on the forward flight problem was the integral analysis of Velkoff,[10] followed by the study of McCroskey and Yaggy.[11] In the latter paper, it was shown that both crossflow and unsteady influence could be handled within the framework of a regular perturbation expansion, and the analysis was applied to simple flow geometries. McCroskey and Yaggy also formulated an approximate method of dealing with the influence of the downwash vorticity, if known, on the inviscid flow near the rotor surface. At a more practical level, Harris et al.[12] recently described a method for predicting overall rotor performance, using the hypothesis that blade stall characteristics can be estimated from yawed-wing and oscillating airfoil data.

In this paper, we shall consider the boundary-layer flow over airfoils with finite thickness and extend the previous work to the region near the axis of rotation. The methods of approach which were taken in the present study‡ were the following: 1) a direct numerical integration of the three-dimensional or two-dimensional time-dependent laminar boundary-layer equations; 2) an extension and re-evaluation of the perturbation analysis of McCroskey and Yaggy;[11] and 3) measurements of separation bubbles and transition on rotating blades and stationary airfoils. The numerical integration is based on the numerical methods developed by Dwyer[14,15] and was employed to study both three-dimensional hover problems and time-dependent two-dimensional flows. The three-dimensional hover analysis includes the flow near the hub for thin airfoils and circular cylinders. The time-dependent investigations simulate the unsteady effects caused by forward flight on the outer portions of the rotor.

The perturbation expansion has been carried out to higher order terms for both rotational and time-dependent influences. Also, the validity of the perturbation work has been completely confirmed by the numerical computations. The re-evaluation of the perturbation solution is the result of a critical study of the separate influences of the crossflow,

‡ Some of the present numerical and perturbation solutions were presented recently in Ref. 13.

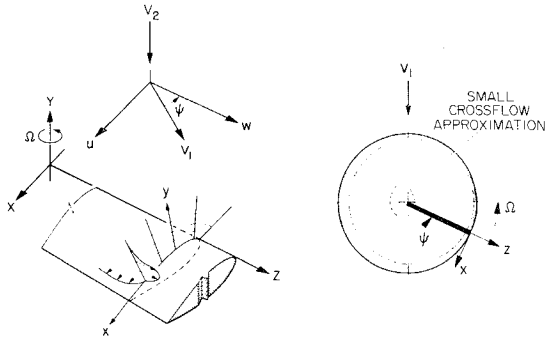

Fig. 1 Coordinates in the rotating system.

Coriolis, centrifugal, and unsteady terms in the boundary-layer equations. This study provides valuable insights for a theoretical understanding of the effects of the various secondary terms on the primary flow over the rotor blade.

The experimental studies utilized blades which were tested in a subsonic wind tunnel as two-dimensional airfoils and yawed wings, and on propeller test stands in pure rotation. The results are not as extensive as the analytical work, however measurements were made of laminar separation and transition to turbulence. The separation studies were patterned after those of Velkoff, Blaser, and Jones,[16] in which ammonia vapor was emitted from orifices and allowed to develop a pattern on ordinary ozalid blue-line reproduction paper. Such traces showed an abrupt change in flow direction just down-stream of the suction peak in the chordwise pressure distribution. Hot wire anemometry indicated that the discontinuity in the ammonia streak is associated with a laminar separation bubble and turbulent reattachment shortly down-stream, very similar to the boundary-layer behavior on two-dimensional airfoils.

Transition patterns were detected by means of subliming films of acenaphthene which gave results similar to those of Tanner and Yaggy.[17] The transition lines determined by the acenaphthene were verified by heated film skin-friction gages, following Bellhouse and Schultz.[18]

II. Analysis and Formulation

The coordinate systems used to study the boundary flow are shown in Fig. 1. The Cartesian axes (X,Y,Z) are aligned with the Y-axis parallel to the angular velocity vector $\mathbf{\Omega}$, and were chosen to be left handed so that the nomenclature would be consistent with standard two-dimensional boundary-layer terminology. A complementary set of curvilinear coordinates (x,y,z) is defined by the airfoil shape and is used to describe the boundary-layer flow. The appropriate laminar, incompressible flow equations for the curvilinear coordinates shown in Fig. 1 have been presented in Ref. 11 and are the following:

Continuity

$$\partial u/\partial x + \partial v/\partial y + \partial w/\partial z = 0 \tag{1}$$

x-Momentum

$$\partial u/\partial t + u\partial u/\partial x + v\partial u/\partial y + w\partial u/\partial z - 2\Omega w\cos\alpha = \nu\partial^2 u/\partial y^2 - (1/\rho)\partial p/\partial x + \Omega^2 X \tag{2}$$

z-Momentum

$$\partial w/\partial t + u\partial w/\partial x + v\partial w/\partial y + w\partial w/\partial z + 2\Omega u\cos\alpha = \nu\partial^2 w/\partial y^2 - (1/\rho)\partial p/\partial z + \Omega^2 Z \tag{3}$$

where α is the angle between the x and X axes, and the pressure gradients are related to the inviscid flow. Also, u, v, and w are the boundary-layer velocities in the x, y, and z directions, respectively; t is the time coordinate; subscript e refers to quantities at the edge of the boundary layer; and ν is the kinematic viscosity.

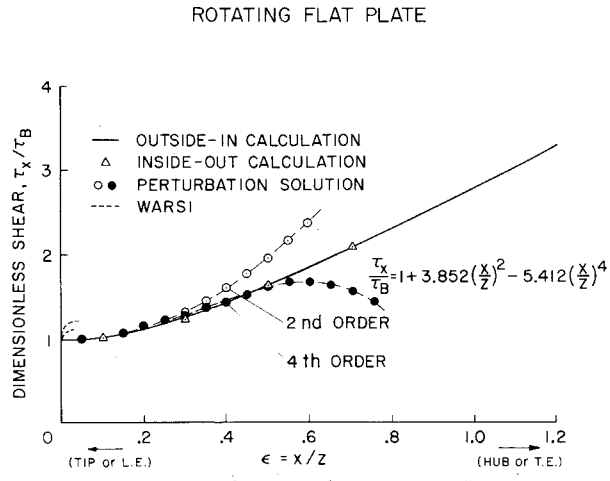

Fig. 2 Comparison of results for primary shear stress on a steady rotating flat plate blade.

The mathematical nature of Eqs. (1–3) is essentially parabolic and both initial and boundary conditions are needed to obtain solutions. (The initial value problem will be discusssed in detail in another section of the paper.) In general, the determination of the boundary conditions from the inviscid flow is difficult for three-dimensional problems, however for the paper, the constant circulation solutions of Sears[1] and McCroskey[11] were employed.

It is convenient to change the dependent variables and transform coordinates before obtaining solutions. The transformations used are,

$$f' = u/U_e, \quad \xi = x, \quad \eta = y(U_e/2\nu x)^{1/2}, \quad \zeta = z, \quad \tau = t \quad (4)$$

If these changes are introduced into the previous equations, the following set of equations are obtained:
Continuity

$$\xi\partial f'/\partial\xi + (\partial f'/\partial\eta)\eta/2(\beta_x - 1) + \partial V/\partial\eta + (\xi/U_e)\partial w/\partial\zeta + \beta_x f' + (\eta/2U_e)\partial w/\partial\eta\beta_z = 0 \quad (5)$$

x-Momentum

$$(\xi/U_e)\partial f'/\partial\tau + \xi f'\partial f'/\partial\xi + \mathbf{V}\partial f'/\partial\eta + \xi(w/U_e)\partial f'/\partial\zeta - (2\Omega\xi w\cos\alpha)/U_e^2 = \beta_x(1 - f'^2) + (\xi W_e/U_e^2)\partial W_e/\partial x - \beta_z f' w/U_e + \tfrac{1}{2}(\partial^2 f'/\partial\eta^2) + \beta_\tau(1/U_e - f'/U_e) \quad (6)$$

z-Momentum

$$(\xi/U_e)\partial w/\partial\tau + \xi f'\partial w/\partial\eta + \mathbf{V}\partial w/\partial\eta + (\xi w/U_e)\partial w/\partial\zeta + 2\xi\Omega f'\cos\alpha = \xi\partial U_e/\partial\zeta + \xi(W_e/U_e)\partial W_e/\partial\zeta + \tfrac{1}{2}(\partial^2 w/\partial\eta^2) + (\xi/U_e)\partial W_e/\partial\tau \quad (7)$$

where

$$V = v(x/2\nu U_e)^{1/2}$$

$$\mathbf{V} = [V + f'/2(\beta_x - 1) + (w/U_e)(\eta/2)\beta_z + (\eta/2)\beta_\tau/U_e]$$

$$\beta_x = (\xi/U_e)\partial U_e/\partial\xi, \beta_z = (\xi/U_e)\partial U_e/\partial\zeta, \beta_\tau = (\xi/U_e)\partial U_e/\partial\tau$$

The advantages of the transformed Eqs. (5–7) are: 1) possible leading-edge singularities along the plane $x = 0$ are removed; 2) equations to determine the initial conditions along $\xi = 0$ may be obtained by taking the limit $\xi \to 0$; and 3) the boundary-layer thickness is very nearly constant in the transformed coordinates. In the perturbation analysis, a slightly different change of independent variables was made, and this change can be found in Ref. 13.

As mentioned previously there are two different types of analytical techniques used in the paper, the perturbation and numerical methods. The perturbation method does not have to tackle the initial value problem explicitly, and its application has been presented in detail in Refs. 11 and 13. The basic features of the method consist of a regular perturbation expansion of the unsteady, three-dimensional equations of motion, employing quasi-steady and small-crossflow approximations to determine the order of magnitude of the terms in Eqs. (5–7). Although its application is limited to rather simple geometric shapes, it can be extremely useful for obtaining a theoretical understanding of the relative significance of various crossflow and unsteady terms. The reason for this usefulness results from the reduction of the number of independent variables from four to two, and from the fact that mostly linear ordinary differential equations are employed in the analysis.

The numerical methods, which were used for the majority of the results of this paper, must tackle directly the initial values problem posed by the equations of motion. Along the plane $\xi = 0$, a set of equations to determine the initial conditions for that plane may be obtained by taking the limit $\xi \to 0$.[14] The equations that result are usually well known and tabulated results can be obtained from standard references, e.g., Ref. 19 (e.g., a sharp leading-edge body will result in a Blasius-type solution at $\xi = 0$). However, along a plane of constant ζ it can be very difficult to obtain initial conditions. In the region $\zeta \to 0$ it is doubtful whether the present set of equations will hold, and over the rotor there is no convenient line of symmetry or region of known velocity. Furthermore, it is known from experiments and approximate solutions that the crossflow velocity is usually radially outward in the bottom regions of the boundary layer, while at the top of the boundary layer the crossflow velocity is usually directed toward the hub. These difficulties forced the development of an approximate technique for obtaining ζ-direction initial conditions.

The method that was employed to obtain the initial conditions was essentially a brute force type. It consisted of assuming the initial velocity profiles at a station of constant ζ, and then iterating with the full boundary-layer equations until a local solution was obtained.[13,20] The assumed velocities were chosen to be the local, steady, two-dimensional boundary-layer ones. For the region of the rotor blade far away from the hub ($X/Z \ll 1.0$), it has been shown by the perturbation method that the u-velocity profile is very close to its two-dimensional value. Therefore, a large value of ζ was chosen to apply the starting procedure. Since the details of the iteration technique varied slightly for the three-dimensional and time-dependent problems, it will be convenient to discuss further details of the starting procedure in conjunction with the solutions to the problems solved.

The finite-difference schemes used for the calculations were similar to those developed by Dwyer.[14] The one difference in the present calculation was the existence of positive and negative crossflow. The negative crossflow does present theoretical and computational problems, and a complete discussion of these problems can be found in Refs. 20 and 28.

III. Results and Discussions

Rotating Flat Plate

To bring out the important features of any flow analysis or solution, it is always convenient to consider a simple geometry. Therefore, the first results to be presented are those for flow over a rotating flat plate. This problem has been considered in detail in Refs. 3, 5, 9, and 11; however, the results were limited to a flow region far from the hub.

The results of the numerical solution of the boundary-layer equations for flow over a rotating flat plate are shown in Fig. 2, along with a new extended perturbation analysis. The numerical calculations were carried out in two different ways. The first method started far away from the hub ($z/c = 6.0$) and proceeded inward, while the second method started at $z/c = 1.0$ and marched outward. Both methods gave results

within ½% of each other, thus indicating that the iterative scheme for starting the calculation worked well. These results also indicate that it is possible to integrate against the flow for some problems and obtain unique results.[22,28] In general, however, numerical calculations of flows with both negative and positive crossflow should be analyzed carefully for nonuniqueness.

Figure 2 shows several other important results. The first is that the numerical results give a direct confirmation of the predictions of the perturbation analysis, both with regard to the magnitude of the wall shear and with regard to the assumed parameters. For small values of $\epsilon = x/z$ (<0.3), the perturbation results carried out to second order $[(x/z)^2]$ are adequate to describe the flow, while the fourth-order results $[(x/z)^4]$ are valid for $x/z \lesssim 0.5$. Also, it is important to note that the character of the flow is completely determined by the single parameter x/z. The reason for this correlation with x/z is that the pressure gradients and Coriolis forces are functions only of x/z in the transformed plane for the flat-plate problem (they are not functions of x/z in the physical plane and that is why the local shear stress is divided by the local Blasius value).

Another important result in Fig. 2 is that the shear stress can become much larger than its two-dimensional value in the region of the hub, although for the range of interest for helicopters ($x/z \lesssim 0.1$) the effects of rotation are very small. The reason for the high shear in the hub region is twofold: 1) an increased crossflow in the bottom regions of the boundary layer; and 2) an induced crossflow pressure gradient from the term $W_e(\partial W_e/\partial x)$. In the vicinity of the hub, the induced pressure gradient term can become very large and its influence can dominate the entire problem, as will be seen in a later section.

A third result in Fig. 2 is a comparison of the numerical and perturbation analyses with those recently published by Warsi.[9] Warsi's numerical results do not correlate with x/z and imply significant changes in wall shear for small x/z, in contrast with both the present numerical and perturbation results.§ Therefore, his results appear to be in error. It should be also mentioned that the amount of computer time involved in Ref. 9 was almost two orders of magnitude larger than the time required to calculate the numerical results presented in this paper.

Additional insight into the flat-plate flow may be obtained by studying the velocity profiles and crossflow velocity derivatives. A comparison of the velocity profiles[13] between the numerical and perturbation solutions shows that they are identical for small x/y, however, when x/z takes on a value of 0.7 there is substantial deviation. Similarly, it was observed that the crossflow derivative was large for large values of x/z near the hub. It is the large crossflow derivative which the perturbation analysis does not handle well, and this derivative is partially responsible for the deviation between the numerical and perturbation solutions. It should be pointed out that the perturbation method does give correct qualitative trends.

Oscillating Flat Plate

In this section the oscillating flow over a flat plate will be described. The analysis will first be restricted to a two-dimensional unsteady flow, and the influence of crossflow due to rotation and forward flight will be neglected. These results are of considerable interest in general studies of unsteady boundary layers. Next the oscillating crossflow that exists on an actual rotor will be added. Since there are four independent variables in this case and the finite-difference program has been limited to three so far, only the perturbation solution is available at this time. However, the accuracy of the perturbation analysis has been explored thoroughly in the three-dimensional steady and two-dimensional unsteady cases, thereby enhancing the confidence that can be placed in the three-dimensional unsteady results.

§ In a subsequent private communication, Prof. Warsi described new results that agree somewhat better with the present results.

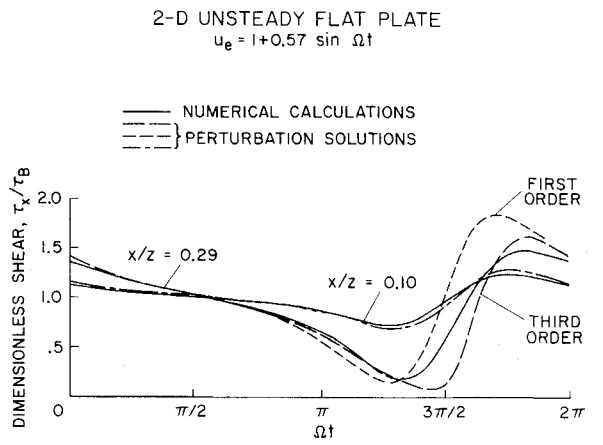

Fig. 3 Comparison of results for shear stress on two-dimensional oscillating flat plate.

The first problem that will be solved is the case of the following oscillating freestream velocity:

$$U_e/U_{av} = 1 + \mu \sin\Omega t$$

Within the framework of the perturbation analysis, the expansion parameter $\epsilon = x/z$ now plays the role of a reduced frequency, $\Omega x/U_{av}$, where U_{av} is the average freestream velocity and is equal to Ωz for the equivalent rotor problem. Also, $\mu = V_1/U_{av}$ represents the ratio of the fluctuating velocity to the average freestream velocity and Ωt can be considered to represent the helicopter azimuth angle ψ.

As in the rotating blade case, the perturbation analysis does not have to handle the initial value problem directly. However, in the numerical method of solution, the initial-value problem must again be tackled directly. The initial conditions at $\zeta = 0$ are obtained by taking the limit $\zeta \to 0$ in Eqs. (5–7), while the conditions at t = constant must be derived from an iteration scheme. Since the first approximation in the iteration was taken to be the steady solution, it was convenient to choose $\Omega t = \pi/2$ as a starting position, where the unsteady pressure gradient, $\partial U_e/\partial t$, is zero and the boundary-layer flow is close to a local steady Blasius flow. With the initial conditions known, the time-dependent viscous calculation can be carried out using the methods developed by Dwyer.[15] A good check on the iterated initial conditions can be obtained in oscillating flows by doing the calculation through more than one cycle and checking for repeatability.

The results of both the numerical and perturbation solutions for the two-dimensional oscillating flat plate are shown in Fig. 3 for $\mu = 0.57$ and two values of ϵ. As in the rotating case, the results can best be summarized by the wall shear; accordingly, Fig. 3 shows the local instantaneous shear for both solutions normalized by the local instantaneous Blasius shear. For $\epsilon = 0.1$ it is clear that the two agree well for all values of $\psi = \Omega t$, just as both rotating solutions agree well for $\epsilon \ll 1$, even though μ has the rather large value of 0.57. It should be noted that the inertia effects tend to "stabilize" the boundary layer, i.e., to increase the fullness of the velocity profile, for $-\pi/2 < \psi\pi/2$ and to "destabilize" the boundary layer for $\pi/2 < \psi < 3\pi/2$. This effect is 90° out of phase with the velocity in the freestream, because of the phase of the unsteady pressure gradient.

To test the perturbation solution further, ϵ was increased to 0.29 while holding $\mu = 0.57$. Now the perturbation analysis yields large errors in the vicinity of $\psi = 3\pi/2$, where the ratio of fluctuating velocity to instantaneous freestream velocity is greater than unity. Even if the expansion is car-

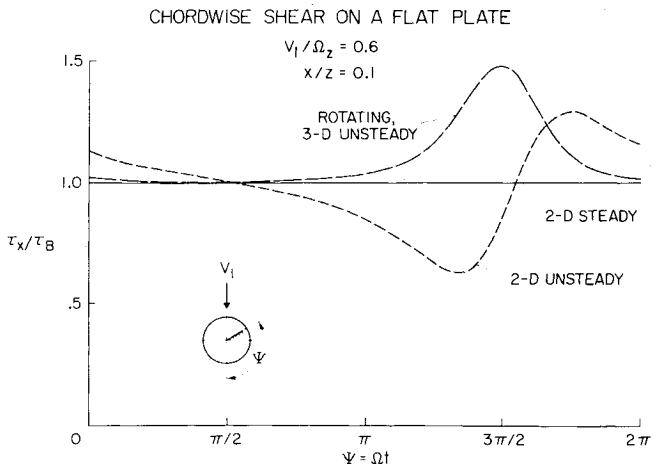

Fig. 4 Primary shear stress on a flat plate blade in forward flight (perturbation solution).

ried out to third order in ϵ, i.e.,

$$\tau/\tau_B = 1 + (2.555\epsilon\mu\cos\psi)/(1 + \mu\sin\psi)^2 + (1.414\epsilon^2\mu\sin\psi)/(1 + \mu\sin\psi)^3 + (0.8158\epsilon^2\mu^2\cos^2\psi)/(1 + \mu\sin\psi)^4 - (1.107\epsilon^3\mu\cos\psi)/(1 + \mu\sin\psi)^4 + (2.112\epsilon^3\mu^2\sin\psi\cos\psi)/(1 + \mu\sin\psi)^5 + (1.136\epsilon^3\mu^3\cos^3\psi)/(1 + \mu\sin\psi)^6 + \ldots \quad (8)$$ ¶

the series converges so slowly at these values of ϵ and μ that poor results are obtained for $\pi < \psi < 2\pi$. On the other hand, the results are very good for $0 < \psi < \pi$, where $\mu/(1 + \mu\sin\psi)$ is small and the series converges rapidly.

In the more specialized and more difficult problem of a flat-plate rotor blade in forward flight, the inviscid crossflow can be much larger than in pure rotation, because of the relative magnitudes of V_1 and $\Omega(\phi - 2X)$. Also there is the further complication of the oscillating sweep angle,

$$\Lambda = \arctan[\mu\cos\Omega t/(1 + \mu\sin\Omega t)]$$

The oscillating crossflow in the boundary layer can be expected to alter the primary flow, and the results in Fig. 4 show that this is indeed true.

It is interesting to compare closely the solid curve in Fig. 4 with the results labeled "$x/z = 0.1$" in Fig. 3. In both cases, the largest changes in wall shear occur for $\pi < \psi < 2\pi$, i.e., on the retreating blade $\epsilon\mu/(1 + \mu\sin\psi) \simeq 0.15$ at $\psi = 3\pi/2$). However, the two-dimensional and three-dimensional results are considerably different for $\pi < \psi < 3\pi/2$, where the crossflow effects couple strongly with the primary flow. The difference in the two results can also be illuminated by comparing the expression for the forward-flight wall shear,

$$\tau_x/\tau_B = 1 - (0.2043\epsilon\mu\cos\psi)/(1 + \mu\sin\psi)^2 + 3.852\epsilon^2/(1 + \mu\sin\psi)^2 - (2.610\epsilon^2\mu\sin\psi)/(1 + \mu\sin\psi)^3 - (1.732\epsilon^2\mu^2\cos^2\psi)/(1 + \mu\sin\psi)^4 + \ldots \quad (9)$$

with the two-dimensional result given by Eq. (8). All of the perturbation terms are of opposite sign in the two cases, indicating that the forward-flight crossflow effects compete with and overpower the inertia effects. Also, the term $3.852\epsilon^2/(1 + \mu\sin\psi)^2$ arises solely due to rotation; it plays an important role in increasing the wall shear in the vicinity of $\psi = 3\pi/2$ for large values of μ.

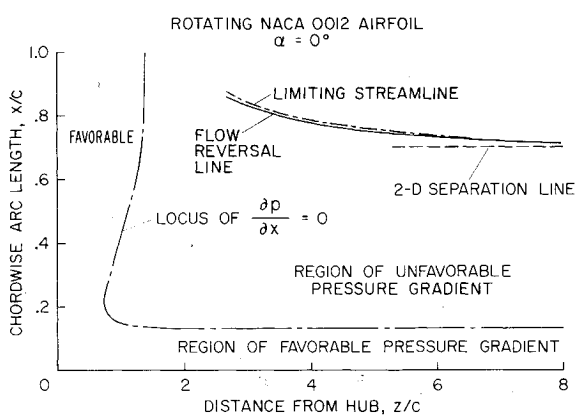

Fig. 5 Effect of rotation on the position of the limiting streamline and flow reversal point for a NACA 0012 airfoil.

¶ The first three terms in Eq. (13) are identical to the result of Moore.[23]

Rotating Airfoils

As is well known, the flow over a flat plate is a drastic simplification of the flow over a helicopter wing. In this section of the paper results of laminar boundary-layer calculations over a finite thickness rotating blade will be presented. The primary purpose of these calculations will be to investigate the importance of crossflow effects compared to the primary flow pressure gradient. Only numerical results and some limited related experimental data will be presented, since the perturbation analysis does not readily lend itself to finite thickness aerofoils.

The rotating aerofoil flow investigated, that over an NACA 0012 aerofoil section, is very representative of contemporary helicopter blades (of course, the calculation is somewhat unrealistic because of the assumption of laminar flow). For the inviscid flow the constant circulation solution of Sears was used for an angle of attack of 0° and the two-dimensional potential function required for this flow as obtained using the method of Theodorsen.[24] It should also be mentioned that the calculations over the aerofoil will only be carried out to the point where the primary flow velocity reverses itself (flow reversal line). Because of the fact that the crossflow velocity is small for this problem, the flow reversal line will be essentially identical to the limiting surface streamline.[19] (The limiting surface streamline divides upstream and downstream fluid at the bottom of the boundary layer.)

Figure 5 shows the results of the calculations for the flow reversal line, as defined previously. Two important features are exhibited in Fig. 5: 1) the flow reversal moves aft as z decreases, and 2) a large rotationally induced pressure gradient exists near the hub. For the 0012 airfoil section, the limiting streamline is behind and very close to the flow reversal line. It is also apparent, that at a distance of about six chord lengths from the hub, the flow reversal line begins to deviate substantially from its two-dimensional value, and near the hub no separation will occur at all. The important influence of the crossflow-induced pressure gradient on separation can be seen by observing the line in Fig. 5 labeled "Locus of $\partial p/\partial x = 0$." This line separates the regions of favorable pressure gradients from regions of unfavorable gradients. For large z, the pressure gradient is favorable near the leading edge of the rotor and then becomes unfavorable past the point of maximum thickness, as in two-dimensional airfoil theory. However, for small z (i.e., close to the hub), the pressure gradient is favorable over the entire blade. The favor able pressure gradient is a direct result of the crossflow-induced pressure gradient, $W_e(\partial W_e/\partial x)$. It seems that this important influence of rotation has not been recognized heretofore, except in Refs. 3–7, and even Liu[5] did not seem to appreciate its importance fully.

Over-all confirmation of the predictions of laminar separation and further insights into the rotor boundary-layer problem are given in Fig. 6. In this figure, the open symbols

show the measured points of laminar separation at $z/c = 2.4$, based on the experimental ammonia-streak discontinuities mentioned in the Introduction. Also shown are the numerical solutions and the measurements of transition to turbulence. The latter was found to be essentially independent of three-dimensional effects and Reynolds number for $Re > 5 \times 10^5$ and $\alpha > 0°$, indicating that the chordwise pressure gradients dominate the transition process for these conditions. Similar data were obtained for NACA 0015 airfoils, differing only in the chordwise location of the separation and transition points.

One of the most important points to be made in connection with Fig. 6 is that the chordwise pressure gradients are so strong at large angles of attack that the effects of crossflow and rotation upon the laminar flow are insignificant at this value of z/c. Thus the analytical and experimental results for separation agree well with the two-dimensional calculations for large α. In agreement with theory and two-dimensional experiments,[25] the laminar flow appears to be independent of Reynolds number.

Another important result is that the transition process for $\alpha \gtrsim 6°$ seems to occur in the free shear layer that develops after laminar separation, and this is followed by turbulent reattachment shortly downstream. This hypothetical flow picture, which corresponds directly to the well-known laminar separation bubble on two-dimensional airfoils, is sketched on the right side of Fig. 6. At lower angles of attack, however, transition to turbulence precedes, and therefore precludes, laminar separation, as indicated in the sketch on the left. The same is true on the lower surface of the airfoil.

Finally, it should be mentioned that the main difference in the rotating and two-dimensional flow occurs within the separation bubble. Here centrifugal forces move the fluid outward significantly; this is how the bubble can be detected by the ammonia technique. After looking closely at the ammonia-trace photographs one is tempted to speculate that the laminar separation line represents an accumulation of surface streamlines, much like the pictures proposed by Maskell[26] for yawed wings. Unfortunately, it was not possible to examine the flow more closely in this regard, either numerically or experimentally.

To conclude this section on rotating airfoils, it should be pointed out that for either thin or thick airfoils, the hub region, where the crossflow effects are important, is not very significant with regard to the over-all performance of conventional propellers and helicopter rotors. However, these influences could have a substantial bearing on the performance of short rotors and ship propellers, where the thrust is generated near the hub.

Time-Dependent Airfoil Flow

In this section, the time-dependent oscillating flow over two-dimensional finite-thickness airfoils will be presented and discussed. The object of the study will be to compare the effect of time-dependent pressure gradients and boundary conditions on finite-thickness airfoils with the flat-plate case of zero thickness. The freestream velocity will be identical to that of the flat-plate case presented previously, and the inviscid flow around the NACA 0012 airfoil will be calculated again using the method of Theodorsen.[24]

Shown in Fig. 7 is the time-dependent location of the flow reversal point on an NACA 0012 airfoil at 0° and 8° angle of attack. The flow reversal point is given in terms of the arc length from the leading edge, and the time coordinate can be related to the forward flight case of the helicopter rotor through Fig. 1.

For time dependent flow the flow reversal or zero shear stress point is not necessarily a good measure of the separation point. Therefore, the separation point as defined by Sears[27] has been calculated. The Sears definition involves finding a dividing trajectory and stagnation point with an observer moving with the separation point. In the present calculations this separation has been found iteratively by first having the observer move with the flow reversal line, and then moving with the calculated separation point. As can be seen from Fig. 7 there is very little qualitative or quantitative difference between the flow reversal and defined separation point for $0 < \Omega t < 3\pi/2$.

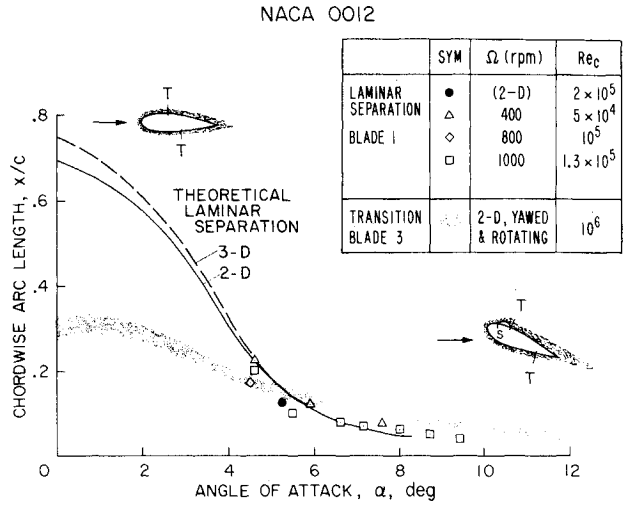

Fig. 6 Separation and transition on a rotating NACA 0012 airfoil.

The boundary-layer numerical calculations were started at $\psi = \Omega t = \pi/2$ since for this point the pressure gradients are independent of time. The iteration process was then applied and the calculations were carried out for three cycles to check for repeatability. As can be seen from Fig. 7, there is very little difference between the time-dependent flow in the region of $\psi = \pi/2$ and steady two-dimensional flow for $\alpha = 0$; therefore, the initial value problem can be posed easily in this region. The region of the flow where the time-dependent influences are the greatest is $\pi \leq \psi \leq 2\pi$. At the point $\psi = \pi$, the unsteady pressure gradients have their maximum adverse value, however, the retardation influence is not the greatest at this point. The reason for this phase shift is that the inviscid velocity is 90° out of phase with the pressure. The potential velocity takes on a minimum value at $\psi = 3/2\pi$, and the combination of this with the adverse pressure gradient causes the minimi in the separation and flow reversal lines to occur between π and $3/2\pi$. A similar circumstance exists for the portions of the oscillating cycle where the unsteady pressure gradients are favorable. The maximum favorable pressure gradients exist when $\psi = 2\pi$; however, the flow reversal line is the farthest from the leading edge for

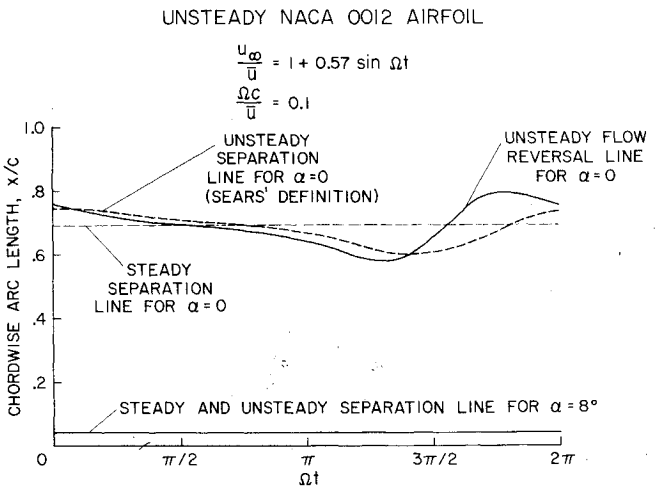

Fig. 7 Effect of unsteady velocity upon "separation" for a NACA 0012 airfoil.

$3/2\pi \leq \psi \leq 2\pi$. Again, the reason for this behavior is the phase differences between the edge velocities and the pressure gradients.

The results for $\alpha = 8°$ are rather striking, in that the unsteady effects have no significant influence upon the position of flow reversal. A similar result was obtained for the circular cylinder under the same flow conditions. For both of these cases, the chordwise pressure gradients are much larger than for the flat plate or the 0012 airfoil at $\alpha = 0°$. Coupled with the results of the previous sections, this seems to suggest that the chordwise pressure gradients tend to dominate the laminar boundary-layer behavior on a helicopter rotor in forward flight. However, this conclusion should be taken very cautiously since the investigation has not looked into the influences of time-dependent angle of attack or time-dependent crossflow on finite-thickness blades.

At this point in the discussion it is appropriate to relate the results of this theoretical investigation of time-dependent aerofoil flow to experimental studies. Probably the most serious deficiency of the study is the inviscid flowfield used, which did not have any time-dependent separation and wake effects included. In a real flow situation the motion of the separation line and the time-dependent structure of the wake will influence the entire flowfield around body. This influence will take the form of pressure gradients imposed on the boundary layer which could be considerably different than the ones used in the present theoretical investigation. Therefore, since a boundary layer calculation cannot be better than the inviscid flow boundary conditions, the present results must be used cautiously when applied to experimental data. However, it has been shown in the investigation that cordwise pressure gradients ($U_e \partial U_e/\partial x$) do dominate over the explicitly time-dependent gradients ($\partial U_e/\partial t$), and therefore a quasi, two-dimensional, steady analysis with the experimental pressure over the aerofoil may be adequate to calculate the boundary-layer flow. The test of this hypothesis will come only after considerably more experimental data become available.

Study of Secondary Terms

The perturbation analysis can, because of the ordering of the forces in terms of the parameters ϵ and μ, provide a basis for a detailed study of the influence of both forward flight and rotation upon the primary flow over a helicopter blade. This analysis has been carried out in Ref. 13, and there it has been shown in general, that the time-dependent influences of forward flight are by far the most important for the helicopter rotor. At the present time an investigation of time-dependent and three-dimensional boundary-layer flow is being carried out numerically, which should give a final verification of the perturbation analysis for the full problem involving rotation and forward flight.

Calculation Time

In this investigation an IBM 7044 digital computing system was used for all the numerical calculations. Even with this relatively slow machine, an average of only 3 min was required to solve the problems presented herein. Therefore, the solution of problems of this type is possible with only limited amounts of computer funds.

IV. Summary and Conclusions

Most of the essential features of laminar boundary layers on rotating blades have been demonstrated by means of relatively simple analytical solutions, which have been verified by direct numerical calculations. The numerical analysis has also provided the detailed structure of the flow near flow reversal for finite-thickness blades. From the results of the investigation the following conclusions can be drawn.

1. The small-crossflow and quasi-study approximations utilized in the perturbation analysis have been verified for the flow over rotating and oscillating airfoil sections, provided the parameters ϵ and $\mu/(1 + \mu \sin\psi)$ are small. Furthermore, the latter restriction is relieved somewhat by the tendency for several of the secondary terms to be mutually cancelling, particularly in the flat-plate case. The conclusions of the perturbation theory apply to helicopter rotor blades and many classes of propellers. However, for the values of $\epsilon = x/z$ appropriate to ship propellers, the small-crossflow approximation does not hold.

2. The initial-value problem inherent in the numerical analysis of rotor boundary layers can be adequately handled by iterative techniques that provide the velocities required to begin the numerical calculations. Also, the previously developed finite-difference methods can be extended to handle the crossflow-reversal situations usually found in rotor problems.

3. The secondary effects which influence the chordwise flow have been identified. Of these the centrifugal force effect appears to be the least important for helicopter rotor blades and slender propellers. The most important effects appear to be time derivatives and crossflow derivatives. Also important are Coriolis forces and apparent pressure gradients induced by the potential crossflow. The latter effect has not been recognized by most previous investigators.

4. The flowfield on a steadily rotating flat plate is uniquely determined by a Blasius-type boundary-layer coordinate and the length ratio $\epsilon = x/z$. For flows on rotating airfoils with pressure gradients, the differences from the two-dimensional solution can be correlated with x/z.

5. The effects of rotation can be important and beneficial with regard to separation of the primary flow in regions of adverse pressure gradients. Since these effects scale with $(x/z)^2$, the maximum benefits accrue closest to the axis of rotation. The unsteady velocity effect has a favorable influence upon separation when U_e is accelerating and an unfavorable one when U_e is decelerating. For a given blade geometry, the unsteady effect is larger than the effects of pure rotation; the ordering of these factors is ϵ and ϵ^2, respectively. In both cases, the influence is largest at small angles of attack.

6. For a helicopter blade in forward flight, there is a substantial inviscid crossflow due to translation, $V_1 \cos\Omega t$, and therefore the boundary layer generally resembles the viscous flow over a swept wing. The perturbation analysis shows that this swept-wing effect influences the primary flow to order ϵ and has a favorable effect with regard to separation on the front half of the rotor disc, i.e., $90° < \psi < 270°$. If the second-order effects are added, the maximum benefits accrue in the third quadrant, $180° < \psi < 270°$.

7. The influence of the strong chordwise pressure gradients on the circular cylinder and the NACA 0012 airfoil at $\alpha = 8°$ was found to almost completely overpower both the rotational and time-dependent effects that were mentioned above. This result was supported by experiments that showed the laminar flow reversal point to agree with two-dimensional calculations. The actual separation appeared to be in the form of a short bubble, followed by an attached turbulent boundary layer.

References

[1] Sears, W. R., "Potential Flow Around a Rotating Cylindrical Blade," *Journal of the Aeronautical Sciences*, Vol. 17, No. 3, March 1950, p. 183.

[2] Fogarty, L. E. and Sears, W. R., "Potential Flow Around a Rotating Advancing Cylindrical Blade," *Journal of the Aeronautical Sciences*, Vol. 17, No. 9, Sept. 1950, p. 599.

[3] Fogarty, L. E., "The Laminar Boundary Layer on a Rotating Blade," *Journal of the Aeronautical Sciences*, Vol. 18, No. 4, April 1951, pp. 247–252.

[4] Tan, H. S., "On Laminar Boundary Layer Over a Rotating Blade," *Journal of the Aeronautical Sciences*, Vol. 20, No. 11, Nov. 1953, p. 780.

[5] Liu, S. W., "The Laminar Boundary Layer Flow on Rotating Cylinders," TN 57-298, June 1957, Air Force Office of Scientific Research, Cambridge, Mass.

[6] Rott, N. and Smith, W. E., "Some Examples of Laminar Boundary Layer Flow on Rotating Blades," *Journal of the Aeronautical Sciences*, Vol. 23, No. 11, Nov. 1956, pp. 991–996.

[7] Graham, M. E., "Calculations of Laminar Boundary Layer Flow on Rotating Blades," Ph.D. thesis, Cornell Univ., Ithaca, New York, 1954.

[8] Himmelskamp, H., "Profiluntersuchungen an einem umlaufenden Propeller," No. 2, Mitteibungen der Max-Planck Institut, Gottingen, Germany, 1950.

[9] Warsi, Z. U. A., "A Numerical Method of Solving the Three-Dimensional Boundary Layer Equations With Application to a Rotating Flat Blade," AIAA Paper 69-227, Atlanta, Ga., 1969.

[10] Velkoff, H. R., "A Preliminary Study of the Effect of a Radial Pressure Gradient on the Boundary Layer of a Rotor Blade," *Proceedings of the CAL/USAAVLABS Symposium on Aerodynamic Problems Associated With V/STOL Aircraft*, Vol. 3, 1966.

[11] McCroskey, W. J. and Yaggy, P. F., "Laminar Boundary Layers on Helicopter Rotors in Forward Flight," *AIAA Journal*, Vol. 6, No. 10, Oct. 1968, pp. 1919–1926.

[12] Harris, F. D., Tarzanin, F. J., Jr., and Fisher, R. K., Jr., "Rotor High Speed Performance-Theory Versus Test," *Journal of the American Helicopter Society*, Vol. 15, No. 3, July 1970, pp. 35–44.

[13] McCroskey, W. J. and Dwyer, H. A., "Methods of Analyzing Propeller and Rotor Boundary Layers With Crossflow," *Symposium on Analytical Methods in Aircraft Aerodynamics*, NASA SP-228, Oct. 1969, p. 473.

[14] Dwyer, H. A., "Solution of a Three-Dimensional Boundary Layer Flow With Separation," *AIAA Journal*, Vol. 6, No. 7, July 1968, pp. 1336–1342.

[15] Dwyer, H. A., "Calculation of Unsteady Leading-Edge Boundary Layers," *AIAA Journal*, Vol. 6, No. 12, Dec. 1968, pp. 2447–2448.

[16] Velkoff, H. R., Blaser, D. A., and Jones, K. M., "Boundary Layer Discontinuity on a Helicopter Rotor Blade in Hovering," AIAA Paper 69-197, Atlanta, Ga., 1969.

[17] Tanner, W. H. and Yaggy, P. F., "Experimental Boundary Layer Study on Hovering Rotors," *Journal of American Helicopter Society*, Vol. 11, No. 3, 1966, p. 22.

[18] Bellhouse, B. J. and Schultz, D. L., "Determination of Skin Friction, Separation and Transition With a Thin Film-Heated Element," *Journal of Fluid Mechanics*, Vol. 24, Pt. 2, 1966, p. 379.

[19] Rosenhead, L., *Laminar Boundary Layers*, Oxford University Press, Great Britain 1963.

[20] Dwyer, H. A., "Hypersonic Boundary Layer Studies on a Spinning Sharp Cone at Angle of Attack," AIAA Paper 71-57, New York, 1971.

[21] Der, J., Jr. and Raetz, G. S., "Solution of General Three-Dimensional Laminar Boundary Layer Problems by an Exact Numerical Method," Paper 62-70, The Institute of Aerospace Sciences, New York, 1962.

[22] Krause, E., "Comment on Solution of a Three-Dimensional Boundary Layer Flow With Separation," *AIAA Journal*, Vol. 7, No. 3, March 1969, p. 575.

[23] Moore, F. K., "Unsteady Laminar Boundary Layer Flow," TN 2471, 1951, NACA.

[24] Theodorsen, T. and Garrick, I. E., "General Potential Theory of Arbitrary Wing Section," TR 452, 1933, NACA.

[25] Gault, D. E., "An Experimental Investigation of Regions of Separated Laminar Flow," TN 3505, 1955, NACA.

[26] Maskell, E. C., "Flow Separation in Three-Dimensions," Rept. Aero 2565, 1955, Royal Aircraft Establishment, Farnborough, Eng.

[27] Sears, W. R., "Some Recent Developments in Airfoil Theory," *Journal of the Aeronautical Sciences*, Vol. 23, No. 5, May 1955, pp. 490–499.

[28] Dwyer, H. A. and McCroskey, W. J., "Crossflow and Unsteady Boundary-Layer Effects on Rotating Blades," AIAA Paper 70-50, New York, 1970.